HEFAT2007
5th International Conference on Heat Transfer, Fluid Mechanics and Thermodynamics
Sun City, South Africa
Paper number: K8

THE FUNDAMENTAL MECHANISM OF SINGLE-PHASE CONVECTIVE HEAT TRANSFER ENHANCEMENT: THE FIELD SYNERGY PRINCPLE AND ITS APPLICATIONS

Yaling-He, Zhiguo-Qu and Wen-Quan Tao*
*Author for correspondence
State Key Lab of Multiphase Flow in Power Engineering, School of Energy & Power Engineering
Xi'an Jiaotong University,
Xi'an Shaanxi 710049
P.R.China,
E-mail: wqtao@mail.xjtu.edu.cn

ABSTRACT

In this keynote lecture a comprehensive review is presented for the field synergy principle (FSP) which was proposed at the 11th International Heat Transfer Conference in 1998 and later further enhanced by many researchers, including the present authors. The lecture is organized as follows. A brief introduction to the FSP is presented in section 1. In Section 2, discussion is given to the indications of the synergy degree between velocity and temperature gradient. In Section 3, numerous examples are provided to show the validity of the principle. In Section 4 a special experimental verification of the principle is provided. In Section 5 numerical examples are provided to demonstrate that the field synergy principle can unify all the existing explanations of single-phase convective heat transfer enhancement. Section 6 is devoted to the applications of the field synergy principle in developing new types of enhanced surfaces for heat transfer. Finally some conclusions are drawn.

NOMENCLATURE

a_t	[-]	turbulent thermal diffusivity, m2/s
cp	[J/(kg·K)]	fluid specific heat
Da	[-]	Darcy number, dimensionless
De	[m]	equivalent diameter
di	[m]	inner diameter of inner tube
do	[m]	outer diameter of inner tube
Di	[m]	inner diameter of outer tube
Do	[m]	outer diameter of outer tube
dp	[m]	particle diameter
dV_i	[m^3]	volume of ith control volume
f	[-]	friction factor, dimensionless
Fc	[-]	field synergy number, dimensionless
g	[m/s^2]	gravitational acceleration,
h	[$W/(m^2K)$]	heat transfer coefficient
H	[m]	distance between two plates
L	[m]	length
$\vec{n}$	[-]	surface unit normal vector
N	[-]	number of control volumes
Nu	[-]	Nusselt number, dimensionless
Pe	[-]	Peclet number, dimensionless
Pr	[-]	fluid Prandtl number, dimensionless
q	[W/m^2]	heat flux
r	[m]	radius, m
Ra	[m]	Rayleigh number, dimensionless
Re	[m]	Reynolds number, dimensionless
S	[m]	arc length along boundary, m
St	[m]	Stanton number, dimensionless
T	[K]	temperature
$\overline{T}$	[-]	dimensionless temperature
Tp	[m]	transverse pitch
U	[m/s]	velocity, m/s
u,v,w	[m/s]	velocity components
x,y,z	[m]	Cartesian coordinates
$\bar{y}$	[-]	dimensionless distance in y-direction

Greek Symbols

β	[K^{-1}]	volume expansion coefficient,
δ	[m]	thickness
∇T	[K/m]	temperature gradient
$\nabla \overline{T}$	[-]	dimensionless temperature gradient,
θ	[-]	synergy angle
ρ	[kg/m^3]	density
ω	[s^{-1}]	rotating angular velocity
Ω	[m^2]	domain

Subscript

f	fluid
in	inlet
m	average
p	particle
t	thermal boundary layer
w	wall
∞	value at great distance from a body

1. INTRODUCTION

The enhancement of convective heat transfer is an everlasting subject for both the researchers and of heat transfer community of academia and the technicians in industry. Numerous investigations, both experimental and numerical, have been conducted and great achievements have been obtained [1-5]. The passive techniques for single phase heat transfer can be grouped usually into three types of enhanced methods:

(1) Decreasing the thermal boundary layer thickness [6,7]. According to this concept, a lot of enhanced surfaces, such as the off-set fin in compact heat exchanger, slotted fin in plate fin-and-tube heat exchangers, are adopted in industries.

(2) Increasing the interruption in the fluids [8,9]. Flow interruption is a well-developed technique to enhance convective heat transfer, and all kinds of inserted devices belong to this type. The rib-roughened ducts adopted in the cooling technique for the turbine blade provide an well-known example.

(3) Increasing the velocity gradient near a heat transfer wall. In [10] for a longitudinally finned tube, an inserted tube was blocked to force all the fluid going through the annulus between the inner tube and outside tube (Fig. 1). The tests have shown that this is an efficient way for enhancing heat transfer both for laminar and turbulent flows.

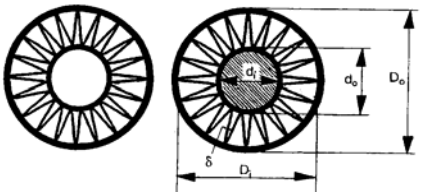

Fig. 1: Centre blocked and unblocked longitudinal tubes

However, up to the end of last century, even for the single-phase flow there was no unified theory which can reveal the essence of convective heat transfer enhancement common to the all enhancement methods. In 1998, Guo and his co-workers proposed a novel concept for enhancing convective heat transfer of parabolic flow [11,12]: the reduction of the intersection angle between the velocity and the fluid temperature gradient can effectively enhance convective heat transfer. Guo's proposal is now briefly reviewed as follows.

For 2-D boundary layer fluid flow and heat transfer along a flat plate with constant temperature, the fluid energy equation takes following form:

$$\rho c_p(u\frac{\partial T}{\partial x}+v\frac{\partial T}{\partial y})=\frac{\partial}{\partial y}(\lambda\frac{\partial T}{\partial y}) \tag{1}$$

where y is the direction normal to the plate. Integrating above equation along the thermal boundary layer, and note that at the outer edge of the thermal boundary $\partial T/\partial y=0$, we have:

$$\rho c_p\int_0^{\delta_t}(\vec{U}\bullet gradT)dy=-(\lambda\frac{\partial T}{\partial y})_{y=0}=q_w \tag{2}$$

In Eq.(2) the convective term has been transformed to the dot production form of the two vectors: velocity and temperature gradient , and the right hand side of Eq. (2) is the heat flux between the solid and the flowing fluid, i.e, the convective heat transfer rate. According to the vector theory, we have:

$$\vec{U}\bullet gradT=\left|\vec{U}\right|\left|gradT\right|\cos\theta \tag{3}$$

where θ is the local intersection angle between velocity and temperature gradient. It is obvious that for a fixed flow rate and temperature difference, the smaller the intersection angle between the velocity and temperature gradient, the larger the heat transfer rate. That is the reduction of the intersection angle will increase the convective heat transfer. According to the Webster Dictionary [13], when several actions or forces are cooperative or combined, such situation can be called "synergy". Thus this idea introduced for enhancing convective heat transfer focuses on the synergy between velocity and temperature gradient and is now called "field synergy principle", and the intersection angle the "synergy angle".

Since most convective heat transfer encountered in engineering are of elliptic type, extending the field synergy principle to elliptic situations is of great importance. Tao et al. [14] proved that this finding is also valid for elliptic flows. Consider a typical elliptic convective heat transfer case—fluid flow and heat transfer over a backward step, as shown in Fig.2. The solid walls are of constant temperature Tw, and fluid with temperature Tf flows into the domain.

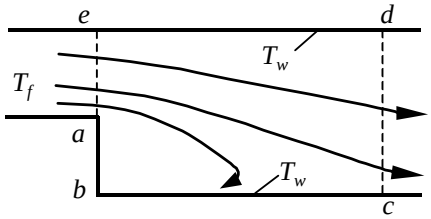

Fig. 2: Heat transfer over a backward facing step

For this case the energy equation reads:

$$\rho c_p(u\frac{\partial T}{\partial x}+v\frac{\partial T}{\partial y})=\frac{\partial}{\partial x}(\lambda\frac{\partial T}{\partial x})+\frac{\partial}{\partial y}(\lambda\frac{\partial T}{\partial y}) \tag{4}$$

By using the Gauss theorem for reduction of the integral dimension the integration of Eq. (4) yields:

$$\begin{aligned}&\iint_{\Omega_{abcdea}}\rho c_p(U\cdot\nabla T)dxdy-\int_{ae}\vec{n}\cdot\lambda\nabla TdS-\int_{cd}\vec{n}\cdot\lambda\nabla TdS\\&=\int_{abc}\vec{n}\cdot\lambda\nabla TdS+\int_{de}\vec{n}\cdot\lambda\nabla TdS=q_{w,abc}+q_{w,de}\end{aligned} \tag{5}$$

where the second and third terms at the left hand side are the heat conduction in the fluids at the inlet and outlet boundaries. According to heat transfer theory[15] when fluid Peclet number (Pe=RePr) is larger than 100(which is often the case in engineering) the heat conduction along fluids can be totally neglected compared with the convective term. This leads to:

$$\begin{aligned}&\iint_{\Omega_{abcdea}}\rho c_p(U\cdot\nabla T)dxdy\\&=\int_{abc}\vec{n}\cdot\lambda\nabla TdS+\int_{de}\vec{n}\cdot\lambda\nabla TdS=q_{w,abc}+q_{w,de}\end{aligned} \tag{6}$$

It is quite clear that a better synergy (i.e., decreasing the synergy angle between the velocity vector and the temperature gradient) will make the integration value larger, i.e., enhancing the heat transfer. It should be noted that even for fluid flow whose Peclet number is less than 100, the first term in the left

hand side of Eq.(5) is still the major one, hence the reduction of the synergy angle between the velocity and the temperature gradient can also enhance heat transfer, though the effect is not so significant as for the case with a larger Peclet number. Thus either for parabolic flows or for elliptic flows, the field synergy principle is valid. The extension of above discussion to three-dimensional cases is very straightforward, and will not be discussed here for simplicity.

Now the meaning of the field synergy principle for the enhancement of single-phase convective heat transfer is summarized as follows [16]: the better the synergy of velocity and temperature gradient, the higher the convective heat transfer rate under the same other conditions. The synergy of the two vector fields implies that (a) the synergy angle between the velocity and the temperature gradient should be as small as possible i.e., the velocity and the temperature gradient should be as parallel as possible; (b) the local values of the velocity and temperature gradient should all be simultaneously large, i.e., larger values of $\cos\theta$ should correspond to larger values of the velocity and the temperature gradient. Better synergy among such three scalar fields($\cos\theta$ and the two modules of velocity and temperature gradient) will lead to a larger value of the Nusselt number. (c) the velocity and temperature profiles at each cross section should be as uniform as possible. The meaning of this point will be further illustrated in the later presentation.

2. INDICATION OF SYNERGY DEGREE

In the application of FSP to develop new enhanced surface of structures, it is often desirable to reveal for an existing heat transfer configuration where the synergy between velocity and temperature gradient is poor, hence improvement is needed. In this regard, the local synergy angle is the unanimous indication. And from the local synergy angle distribution, we can obtain a domain averaged one. A question may arise as what is the appropriate definition to compute the domain-averaged synergy angle. In the past years we tried several definitions, for example

(1) Simple arithmetic mean

$$\theta_m = \frac{\sum \theta_i}{N} \tag{7}$$

where N is the number of control volumes of the entire domain, and θ_i is the local synergy angle.

(2) Volume-weighting mean

$$\theta_m = \frac{\sum \theta_i dV_i}{\sum dV_i} \tag{8}$$

where dV_i is the volume of ith control volume.

(3) Domain integration mean

$$\theta_m = \arccos \frac{\sum |\vec{u}| \bullet |gradt| \bullet \cos\theta_i \bullet dV}{\sum |\vec{u}| \bullet |gradt| \bullet dV} \tag{9}$$

This equation can be written in an equivalent way

$$\sum |\vec{u}| \bullet |gradt| \bullet dV \cos\theta_m = \sum |\vec{u}| \bullet |gradt| \bullet \cos\theta_i \bullet dV \tag{10}$$

when every local synergy angle takes the value of θ_m, the left hand side equals the actual convective heat transfer representing by the right hand side. Thus the cosine of this average synergy angle is the mean value of the domain integration for the local cosine value.

The above different definitions have been applied to several single phase flow situations, including gas and liquid. Fortunately, except the first definition, the averaged synergies from the different definitions have the same variation trend, though different in absolute values. This gives us quite wide flexibility to adopt a definition for the domain averaged synergy angle. Because when the averaged Thus Eqs.(8) and (9) are recommended to adopt.

From the synergy angle, two limitation cases may be deduced, i,e, the one where all the local synergy angle equals zero and the other where the velocity is normal to the temperature gradient everywhere[14]. Such two extreme situation are illustrated in Fig. 3. Case (a) of Fig. 3 is the best one for which heat transfer rate is just proportional the fluid velocity, while case (b) of Fig. 3 is the worst one, for which heat transfer between fluid and solid surface is zero and the fluid motion does not make any contribution to heat transfer. These two cases will be called hereafter the first and second deductions of the FSP .

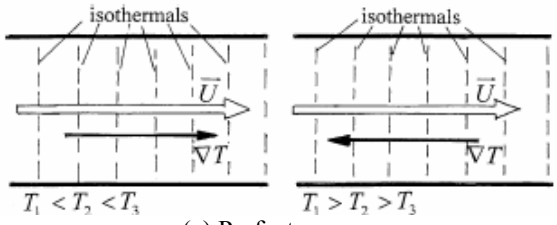

(a) Perfect synergy

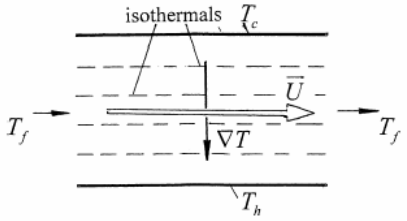

(b) The worst synergy

Fig. 3 Two limit situations of the synergy between velocity and temperature gradient

3. SOME NUMERICAL AND EXPERIMENTAL EXAMPLES SHOWING VALIDITY OF FSP

Numerous numerical and experimental verifications have been conducted to demonstrate the validity of this principle. Followings are some typical examples.

3. 1 Numerical Results of Laminar Flow across a Single Finned Tube

For air flow across a finned tube shown in Fig.4(a), if one unit is taken as a representative, a computational domain can be formed by the body-fitted coordinates as shown in Fig.4(b). Numerical results are obtained at different oncoming flow velocity for finned tube and bare tube without fins[17]. The

velocity and temperature isothermal distributions are presented in Figs. 5 and 6 for bare tube and finned tube respectively.

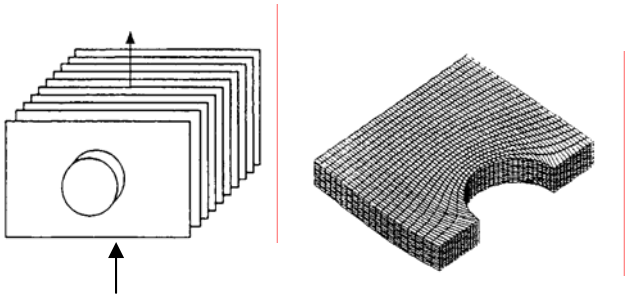

Fig.4 Air flow across a fined tube

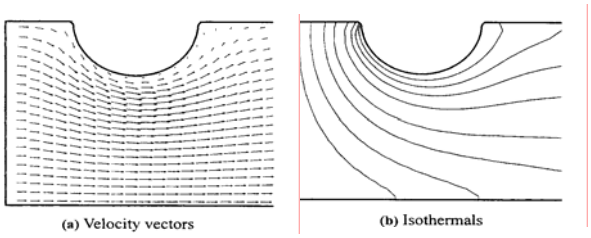

Fig. 5 Results for bare tube without fins (U=0.02m/s)

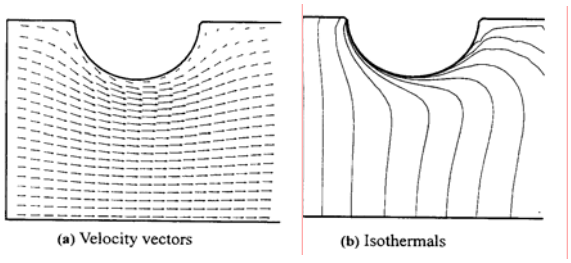

Fig. 6 Results for finned tube(U=0.06 m/s)

It can be clearly observed from the above two figures that the fin not only increases the heat transfer surfaces, but also greatly improves the synergy between velocity and temperature filed. The domain averaged synergy angle for the finned tube is about forty degrees less than the bare tube situation (from 61.7 degrees at U=0.02 m/s to 23.6 degrees at U=0.06 m/s). When the unit averaged Nusselt numbers of the finned tube are correlated by the form of $Nu = c\,\mathrm{Re}^n$, it is found that at low oncoming velocity the exponent n is nearly equals one, indicating a very good synergy between velocity and temperature gradient. With the increase in the oncoming velocity, the vortex formed behind the tube gradually deteriorates the local synergy, and the value of the exponent reduces accordingly. Table 1 represents the results.

Table 1 Variation of the exponent n with Re

Re	*c*	*n*
10 ~ 100	0.034 8	0.998 2
100 ~ 200	0.055 6	0.899 1
200 ~ 400	0.163 8	0.698 6
400 ~ 800	0.362 0	0.566 0

From this example we can withdraw two important conclusions. First, the role of fin does not limited to the increase of heat transfer surface, but also to improve the synergy which has never been discovered before. Second, when velocity and temperature gradient is in very good synergy, the heat transfer coefficient almost increases linearly with the flow velocity.

3. 2 Experimental Results of Laminar Heat Transfer in a Centrifugal Fluidised Bed

Experimental measurements were conducted in [18] for the heat transfer of discrete particles contained in a centrifugal fluidised bed. Analysis has shown that when the rotation number is below some value, the velocity and temperature gradient in the bed are parallel which is the best synergy situation, and hence Nusselt number should be proportional to Reynolds number. This conclusion has been proved by the experiments [18]. Figure 7 presents the measured results.

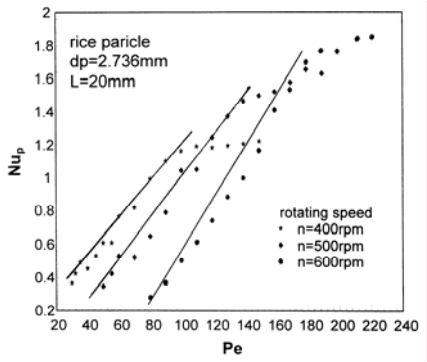

Fig. 7 Variation of Nusselt number vs. Peclet number

It can be seen that at each rotation speed, there is a critical Peclet number (or Reynolds number), below which the particle Nusselt number varies linearly with Peclet number. In this linear variation range, a correlation can be obtained as follows:

$$Nu_p = 0.00242 Pe \left(\frac{L_0}{d_p}\right)^{-0.647} \left(\frac{r_0\omega^2}{g}\right)^{-0.152} \qquad (11)$$

3.3 Numerical Results of Turbulent Heat Transfer Across Parallel Plates

Numerical simulations were conducted in [19] for turbulent air flow across an array of parallel plates shown in Fig. 8. The effect of the plate thickness, δ, was studied by using the low-Reynolds number $k-\varepsilon$ model. The variation of the cycle average Nusselt number with Reynolds number is illustrated in Fig. 9 with plate thickness as a parameter. The characteristic length of the Nusselt number and Reynolds number was $2T_p$. For the case studied, the increase in the plate thickness leads to the enhancement of heat transfer. The predicted domain average synergy angles are presented in Fig. 10. It can be clearly observed that the increase in the plate thickness improves the synergy between velocity and temperature gradient, hence, enhances the heat transfer. These results show that the FSP also applicable to the turbulent heat transfer situation.

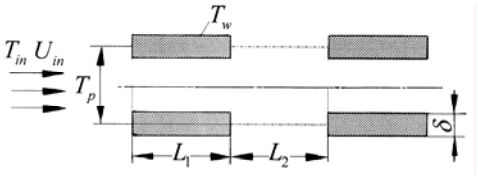

Fig. 8 Turbulent air flow across an array of parallel plates

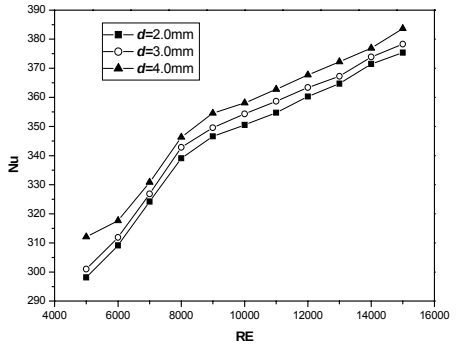

Fig. 9 Plate thickness effect on heat transfer

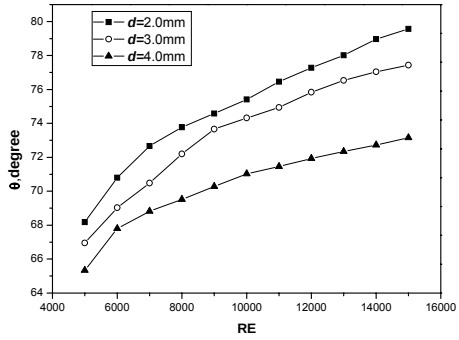

Fig. 10 Variation of domain averaged synergy angle

3.4 Numerical Examples in Rotating Ducts

All the above examples are obtained for static solid surfaces. In [20] numerical predictions were performed for laminar flow and heat transfer in a rotating duct. Two rotating ducts were investigated, these were radial rotation and axial rotation (Fig. 11). By varying the rotation number, defined by:

$$Ro = \omega D_e / u_m \tag{12}$$

where ω is the rotating angular velocity its effect on the duct average Nusselt number was investigated. The results are presented in Fig. 12. From Fig. 12 it can be found that the variation trends of the duct average Nusslet number with the rotation number are in fully consistent with the FSP. A question may arise as far as Fig. 12(d) is concerned: the variation of the domain average synergy angle is so small that its effect might be negligible. The fact is that in the range of an angle more than 80 degrees a minor change may lead to an appreciable variation in its cosine value. For example, cosine of 84.9 degrees=0.08889, while cosine of 84.1 degrees =0.1028, and the variation is more than 10 percentage.

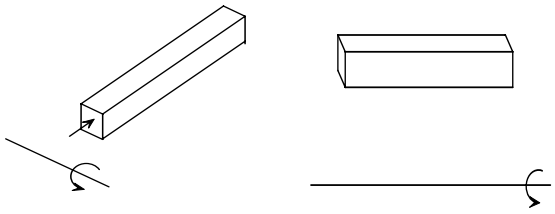

(a) Radial rotation (b) Axial rotation

Fig. 11 Two types of rotating ducts

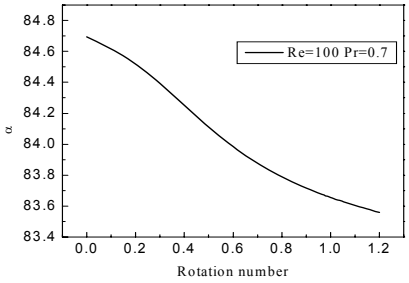

(a) Nu vs Ro of radial rotating

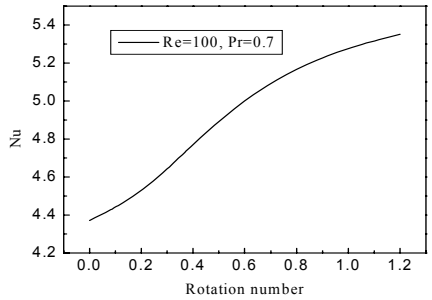

(b) θ vs Ro of radial rotating

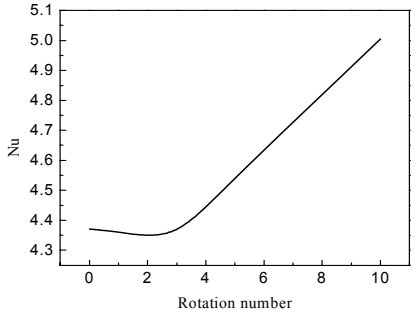

(c) Nu vs Ro of axial rotating

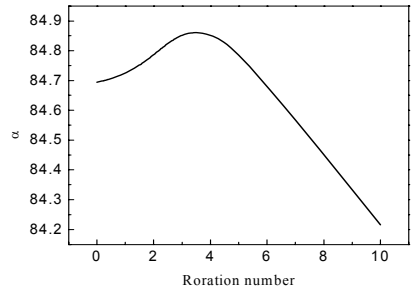

(d) θ vs. Ro of axial rotating

Fig. 12 Heat transfer in rotating ducts

3.5 Why the longitudinal Vortex Can Enhance Heat Transfer

The vortex generator (VG) is an effective method to enhance heat transfer. It can be directly punched out from the fin surface to generate the secondary flow. The vortex may be divided into transverse vortex (TV) and longitudinal vortex (LV) according to the vortex rotating direction. The TV's rotating direction is normal to the main flow (stream wise) direction. The flow with TV may be a pure two-dimensional flow. The LV's rotating direction is the same with the main flow direction. LV is always three-dimensional due to fact that the flow spirals around the main flow direction, and the flow structure is very complicated. The first literature reporting the longitudinal vortex in boundary layer control was presented by Schubauer et. al[21]. Johnson et.al [22] firstly reported the research on heat transfer related to VG. After their work, the study on the heat transfer enhancement in compact heat exchanger by vortex generators has received enormous attentions and some typical results may be found in [23-27].

The traditional viewpoint of the reasons of the heat transfer augmentation with LVG are attributed to that the generated longitudinal vortices disturb, swirl and mix the fluid flow, break the boundary layer developing and thin it. Numerical simulations were conducted in [28, 29] for a rectangular duct with or without a pair of LVG, and the results definitely show that the basic mechanism of heat transfer enhancement of LVG is the improvement of synergy between velocity and temperature gradient.

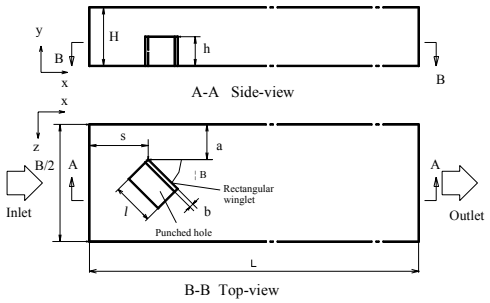

Fig.13 Schematic diagram of the channel with RWLVG

In Fig.13 The schematic view of the half duct with a LVG is shown[28]. A pair of rectangle winglet (RWLVG) are punched from the duct wall in the upstream part of the duct , hence a rectangle hole is formed at the duct bottom as shown in the figure. The duct cross section is rectangular in shape with width B and height H. The attack angle of the winglet, β , is varied from 15 degrees to 90 degrees. The cross section of $B \times H$ is 160X40mm. The length of the channel is 400mm. The thickness of the LVG is determined to be 4mm. The height of the rectangular LVG is 20mm that is one half of the channel height, its length is 40mm. The location of RWLVG is determined by the coordinates of s(=80mm)and a(=10mm) as shown in the figure. Thus the RWLVG is located in the developing flow region. In Fig. 14 a pair of longitudinal vortex are predicted for Re=1600 and $\beta = 30^{\circ}$ and shown at three cross sections of x=0.12m (next to the trailing edge of RWLVG.), 0.20m and 0.28m. Figure 15 presents the ratio of the averaged Nusselt number , Num/Nuo, and the average synergy angle of the duct ,where Nuo is the average Nusselt number of the corresponding plain duct without the LVG. From the figure it can be observed that with the increase in the attack angle the average Nusselt number increases first , reaches its maximum at $\beta = 45^{\circ}$, and then deceases. And when the vortex becomes a transverse one ($\beta = 90^{\circ}$), the heat transfer enhancement is the least among the six cases studied. In the order of the attack angle, the average Nusselt numbers are ranked as $Nu_{m,15} < Nu_{m,30} < Nu_{m,45} > Nu_{m,60} > Nu_{m,90}$. It is very interested to note that the average synergy angles are ranked just in the opposite way, that is: $\theta_{m,\,plain\ duct} > \theta_{m,15} > \theta_{m,30} > \theta_{m,45} < \theta_{m,60} < \theta_{m,90}$. This numerical results definitely show that all the possible explanations for the enhancement mechanism of LVG inevitably can be summarized by the improvement of synergy between velocity and temperature gradient.

More numerical and experimental verification examples may be found in [30].

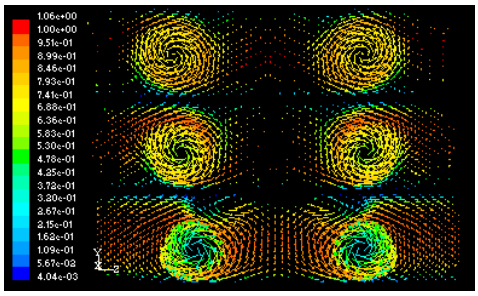

Fig.14 Longitudinal vortices at the different cross sections (x in m)

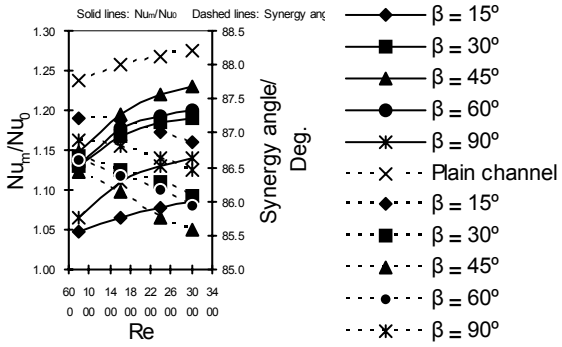

Fig.15 Nu_m / Nu_0 and synergy angle vs Reynolds number for the six cases

4. SPECIAL EXPERIMENTAL VERIFICATION OF FSP

4.1 Two important Deductions from FSP

Conventionally convective heat transfer is understood as the heat transfer between solid surface and fluid moving along

its surface, and the larger the fluid velocity the greater the heat transfer rate. According to the FSP, not all moving fluids can transfer thermal energy with its contacting surface. The necessary and sufficient condition is that the moving fluid temperature gradient must not be normal to its velocity. According to this principle, the reduction of the intersection angle between fluid velocity and temperature gradient is the fundamental mechanism for enhancing convective heat transfer. The most perfect case is the one where the intersection angle is zero in the entire flow domain in which the Nusselt number is proportional to the Reynolds number (first deduction), and the worst case is that the flow velocity is everywhere normal to the local temperature gradient for which the fluid flow doesn't make any contribution to the convective heat transfer no matter how fast the fluid is moving (second deduction).The experimental results in [18] give a strong support to the first deduction of FSP. However, to the authors' knowledge, the second deduction from the FSP has never been experimentally verified. In order to validate such a basic concept of FSP, a special test equipment was designed and some preliminary experiments were performed in the authors group.

4.2 Challenges in the design of test facility

The design of such an experiment is of a great challenge. The major difficulty is to create such a flow field which is everywhere normal to fluid temperature gradient. Having stimulated from some numerical simulations, we decided to establish an axial flow within a square duct whose two lateral walls are maintained at constant but different temperatures, while the other two walls are adiabatic. In such case there will be global temperature gradient from the hot wall to the cold one, whose direction is normal to the axial flow. If the idea of the FSP is valid, then the heat transfer rate from the hot wall to the cold wall of the duct will only be dependent on the temperature difference of the two walls, but nothing to do with the axial flow velocity. In the implementation of the conceptual design, we met the second difficulty. In order to create a fluid temperature gradient which is always normal to the axial fluid flow, the two lateral walls have to be isothermal, otherwise an axial temperature gradient in fluid will exist, which violates the normal condition of the two vectors. This requirement discarded the possibility of using electrical heating for the hot wall. Thus for both hot wall and cold wall fluid heating or cooling have to be used. Then the second difficulty comes. In order to measure the heat transfer from the hot wall to the cold wall more accurately, we need a higher temperature difference between fluid inlet and outlet of each wall. However, from the isothermal requirement, this difference should be as small as possible. Finally we make some compromise between the measurement accuracy and the normal condition: the temperature difference of both the heating water and cooling water are allowed only about 1 degree Celsius, and this one degree difference is taken place in an axial direction as long as 2 meters. In the execution of test one more difficulty (third difficulty) occurred. In the preliminary test the third difficulty as mentioned above occurred. In the measurement of the heat transfer rate, we required that this amount of heat calculated from the heating water and from the cooling water should the same, or their deviation should be within about 5%. However, the required deviation was hardly satisfied, and often the heat transfer from the hot wall was larger than that of the cold wall. After examining many possible factors, we finally realized that apart from the natural heat transfer in the enclosure, there are heat transfers at the outside surface of the two vertical walls by both natural convection and radiation. When the absolute value of the temperature difference of the outside surface of the hot wall and cold wall are not equal, this additional heat transfer rate of the two vertical surfaces are not equal. The hot water within the channel of the hot wall actually released heat to two sinks: one to the environment, and the other to the moving air in the duct. On the other hand the cold water in the channel of cold wall absorbed heat from both environment and from the moving air in the duct. In order that the combined natural convection of the hot wall and the cold wall have the same amount of heat transfer, following conditions are required; (1) the mean temperature of the duct flow should be the same as the environment; (2) and the temperature of the hot wall and that of the cold wall should apart from the environment temperature the same value but in opposite direction. Only when the test procedure is in such condition, the heat balance between the hot wall and cold wall is quite satisfactorily. In the following the specially designed test facility is presented

4.3 The test facility and experimental results

As shown in Figs. 16,17 a long duct composed of two isothermal walls and two adiabatic walls is horizontally positioned and air is flowing through the duct driven by a drawer. The two vertical walls are cooled or heated by two water jackets with a channel thickness of 5 mm through which hot/cold water are going through. The inlet and outlet water temperature difference through each jacket is limited about 1 $^{\circ}$C and the water temperature difference between the two jackets is about 20-50 $^{\circ}$C , therefore the two vertical duct walls can be regarded being kept at constant temperature. When the air is going through the duct and the hot and cold waters are going through the jackets, such an nearly ideal case is formed that the velocity is normal to the fluid temperature gradient which is from hot wall to the cold wall. According to the FSP, the axial velocity of the air does not make any contributions to the heat transfer across the duct. In other words, the heat transfer across the duct is only dependent on the Rayleigh number ($Ra = g\beta\Delta TL^3/a\nu$) but independent on the Reynolds number for which the axial velocity is used. Some preliminary test results are presented in Fig. 18. From the figures, following features may be noted. First, the total heat transfer rates at the two levels of the wall temperature differences are mainly independent on the streamwise flow rate. It is to be noted that the low end of the Reynolds number is actually zero. This implies that within a wide variation range of the streamwise velocity the heat transfer across the main stream is basically not affected. Second, at the two wall temperature difference levels, the heat transfer rates are different; with the higher temperature difference corresponds to a higher heat transfer rate. Third, the energy balances between the hot wall and cold wall are generally good, with the deviation being increased with the

increase in wall temperature difference. In all runs the energy balance may be regarded being within 4.0%. Fourth, in the two heat transfer rates from hot and cold walls, the heat transfer rate from the cold wall, Qc, increases a bit more appreciably with the streamwise flow direction while that from the hot wall is remained unchanged within the measurement uncertainty because of the condensation effect on the cold wall whose temperature is lower than the ambient air. Even though there are some inevitable measurement errors, the test results have demonstrated the second deduction of FSP. For details, reference [31] may be consulted.

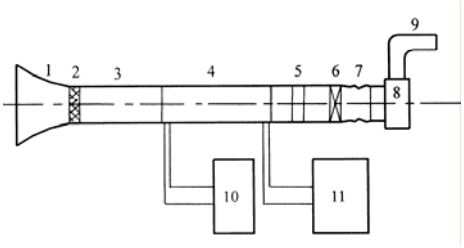

Fig. 16 Schematic diagram of the test system

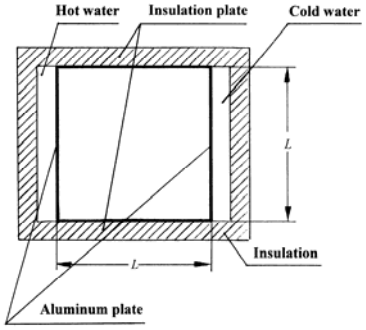

Fig. 17 Cross section view of the test duct

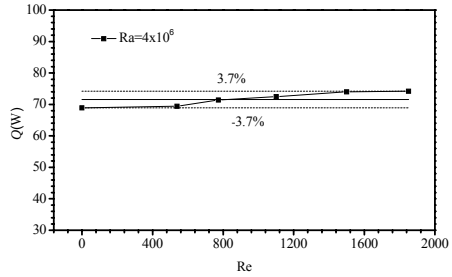

(a) Ra=4x10^6, ΔT=20℃

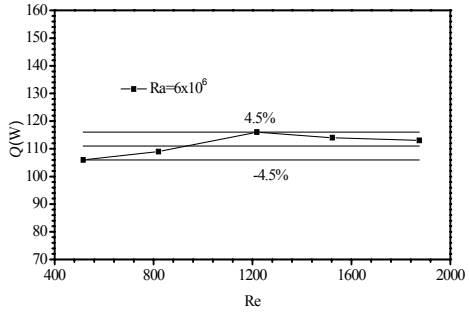

(b) Ra=6x10^6, ΔT=30℃

Fig. 18 Validation test for the second deduction of FSP

5. A UNIFIED MECHANISM FOR ENHANCING SINGLE-PHASE CONVECTIVE HEAT TRANSFER

The three basic enhancement mechanisms of single phase convective heat transfer were presented in Section 1. In [32] it has been shown that all these three mechanisms can be unified by the FSP. The numerical demonstrations are now briefly presented.

5.1 Decreasing Boundary Layer Thickness Equivalent to Reduce the Synergy Angle

Computations were conducted for air flow over a flat isothermal plate and the results for Re=600 are presented in Fig.19, where the characteristic length of Re is the entire plate length. In the figure the variations of the local heat transfer coefficient (LHTC), the integration of the convective term at each cross section (Int) and the cross section averaged synergy angle with the distance from the leading edge are shown. It can be clearly identified that with the increase in x, both Int and LHCT reduces while the section averaged synergy angle increases. This implies definitely that decrease of the thermal boundary layer is inherently related to the reduction of the synergy angle.

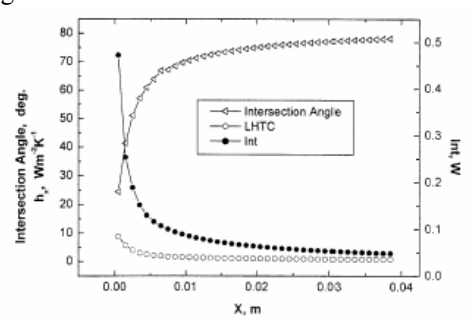

Fig. 19 Variation of Int LHTC and θ_m with x

5.2 Increasing the Disturbance in Fluids Corresponding to Reducing the Synergy Angle

Increasing the disturbance in fluids has been adopted widely as one of the major techniques for enhancing convective heat transfer. In order to simulate such two situations were designed: one without external disturbance and the other with external disturbance while all other conditions remain the same. As shown in Fig. 20 in a parallel plate channel two cylinders with rectangle cross section are inserted. The two cylinders are thermally adiabatic by setting its thermal conductivity almost equals zero (a very small number), the only function of the two cylinders is to increase the disturbances in the fluid. The numerical results for the case of L/H=2, p/h=1.35, h/H=1/3 are presented in Figs.21, 22 and 23. In Fig. 21 the domain integration of the convective term are presented. It can be noted that the Int value of the parallel plate blocked by two inserts (PPDB) is appreciably higher than that of PPD. The duct averaged Nusselt numbers are illustrated in Fig. 22, where two features may be noted. First, the Nusselt number of PPDB is much higher than that of PPD; Second, for Re beyond 400, the two Nusselt numbers keep almost constant, while below this

Reynolds number the value of PPDB Nu decreases with the decrease in Re. It is in this low Reynolds number (hence, low Peclet number) the heat conduction in fluids gradually plays a role. For the PPDB the disturbance only increases the thermal energy transferred by fluid motion, but does not promote the thermal conduction. Therefore when the convective part is absolutely predominant, Nu of PPDB keeps constant, and with the decreasing of Re, the value of Nu gradually decreases. The variation of the domain averaged synergy angle of the two ducts are presented in Fig. 23. The angle of PPDB is about 8-10 degrees less than that of PPD, definitely indicating that increase of fluid disturbance actually means improvement in synergy.

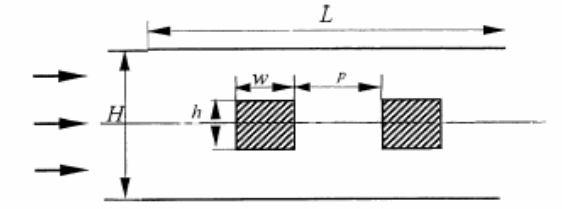

Fig. 20 Parallel plate ducts with two inserts

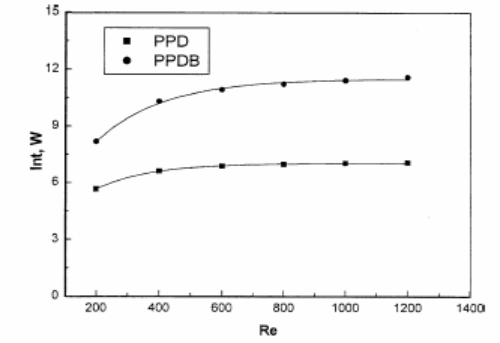

Fig. 21 Domain integration of two cases

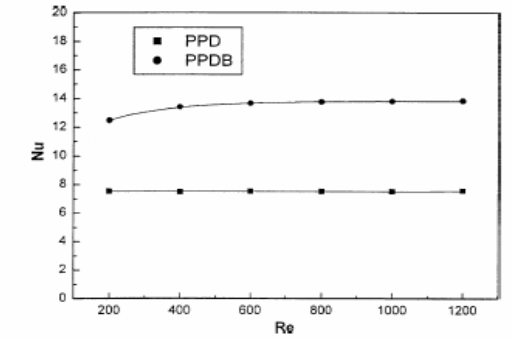

Fig. 22 Nusselt number variations of the two cases

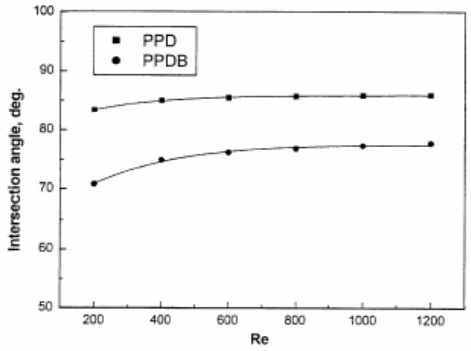

Fig. 23 Domain averaged synergy angle

5.3 Increasing in Wall Velocity Gradient Leading to Improvement in Synergy

To reveal the fundamental reason of why increase the wall velocity gradient can enhance heat transfer, a special numerical simulation was designed. As shown in Fig. 24, for a tube with diameter D, a solid bar with length L2 was inserted. Simulations were conducted for the entrance region for both the smooth tube (ST) and the tube blocked (TB). For comparison, the Reynolds numbers of the two cases were calculated by the same definition, for which the cross averaged velocity at the empty part was used. Therefore, the Reynolds number can be used as the abscissa for both the tubes. The domain integration of the convective term, the domain averaged Nusselt number and the domain averaged synergy angle are presented in Figs.25, 26 and 27, respectively. As for the above case, numerical results reveals that the increase in the velocity wall gradient appreciably improve the synergy (the reduction of domain averaged synergy angle is larger than 10 degrees), hence , can enhance heat transfer.

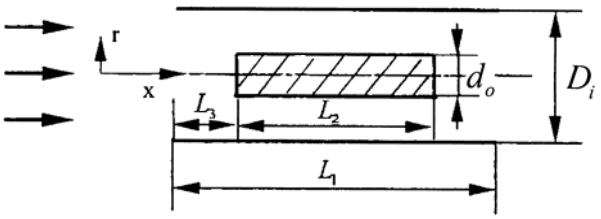

Fig. 24 Tube with a solid bar insertion

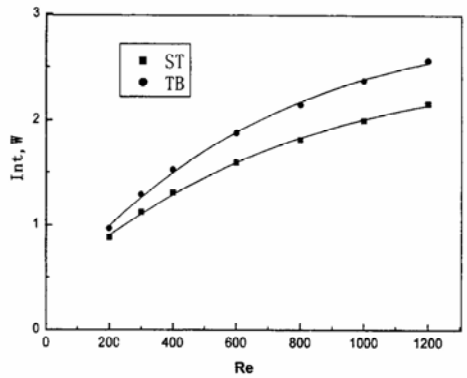

Fig. 25 Domain integration of the convective term

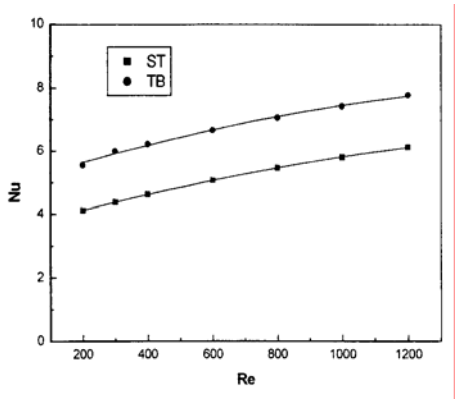

Fig. 26 Domain averaged Nusselt number

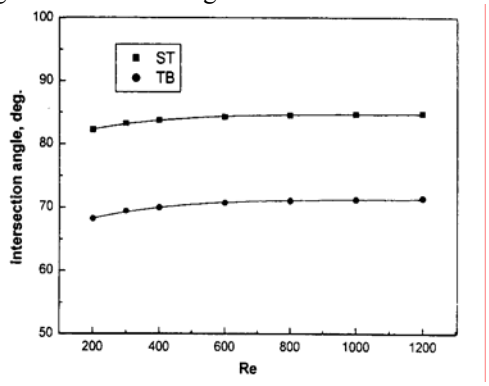

Fig. 27 Synergy angle vs Re

6. APPLICATIONS OF FSP IN DEVELOPING NEW TYPES OF ENHANCED SURFACES

Now attention is turned to the development of new types of enhanced heat transfer surfaces by application of the field synergy principle. Several new enhanced structures were designed under the guidance of FSP and are now used in some industries of China. The major three ones are introduced as follows.

6.1 Slotted Fin Surface with Strips Positioned according to the rule of Front Sparse and Rear Dense

Air-side heat transfer resistance often covers the major part of the total resistance in many over all heat transfer process, hence, enhanced techniques are adopted. The most widely used enhanced configuration is the plate fin-and-tube surface. To further enhance heat transfer, slotted fin may be used. The conventional design of slotted fin surface has regular and uniform distribution of strips as schematically shown in Fig. 28 by pattern 1. Such regular position of strips looks fine, but not efficient and reasonable. Our numerical simulation for a two-row tube plate fin surface reveals that in the inlet part of the fin(i.e, the front part), the fluid isothermals are almost normal to the local velocity (Fig. 29(a),(b)), hence the synergy is very good. However, in the rear part of the fin, synergy becomes worse because of the formation of the fluid vortex. It is this part that enhanced techniques are highly desired. Therefore the strips should mainly be located in the rear part of the fin and in the place where the main stream of gas goes through, as shown by the patter 2 in Fig. 28

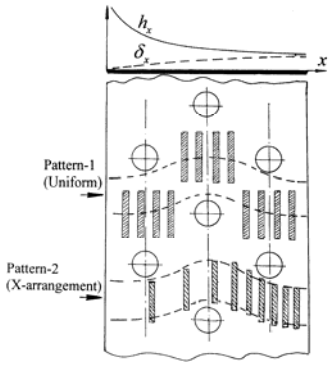

Fig 28 Two patterns of strip position

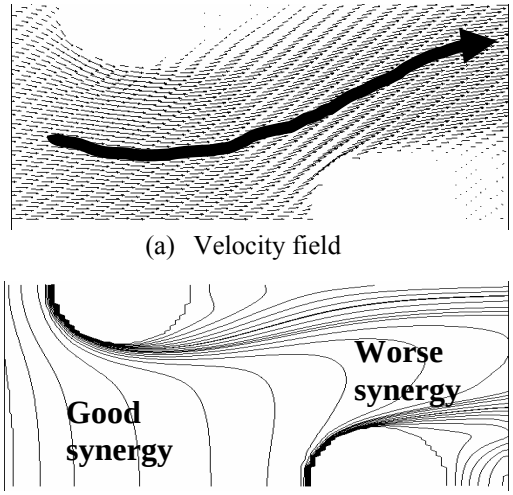

(a) Velocity field

(b) Isothermals

Fig. 29 Velocity and temperature fields of a two-row plate fin-and-tube surface

Based on the above study for air flow across three-row tube finned surface some specially designed slotted fin surfaces are numerically investigated with the strips position according to the rule of "front sparse and rear dense" as shown in Fig. 30 [33]. Numerical simulations were used to find the best configuration. Figure 31 presents a comparison of the Nusselt numbers for three versions of slotted fin under the identical pumping power constraint. The superior performance of the parallel slotted fin studied is very obvious. The three arrangements of the strips along the flow direction all abide by the rule of front sparse and rear dense. However, minor difference exists from one arrangement to the another in the distance between two adjacent strips along the flow direction. Figure 32 is the results of the domain averaged synergy angle. It can be seen that version 3 has the smallest synergy angle, hence was selected as the desired slotted fin surface.

Experiments were conducted for two heat exchangers, one with plain plate fin and the other with the slotted fin of version 1(Fig. 30(b)). The overall heat transfer coefficients and the air-side pressured data are presented in Fig. 33. Compared with the heat exchanger with plain plate fin, the increase in the overall heat transfer coefficient of the slotted fin heat exchanger is at least 26%, while the increase in air side pressure drop is at most

22%, showing very good performance of the designed fin surface.

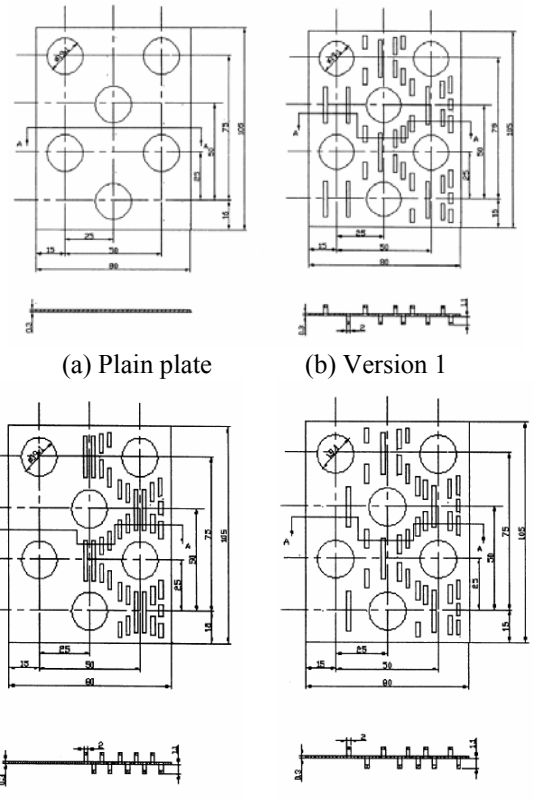

(a) Plain plate (b) Version 1

(c) Version 2 (d) Version 3

Fig. 30 Plain plate fin and three versions of slotted fin designed with the front sparse and rear dense rule

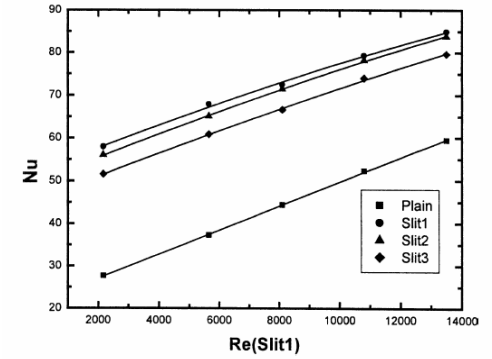

Fig. 31 Predicted Nusselt number of four types of fin

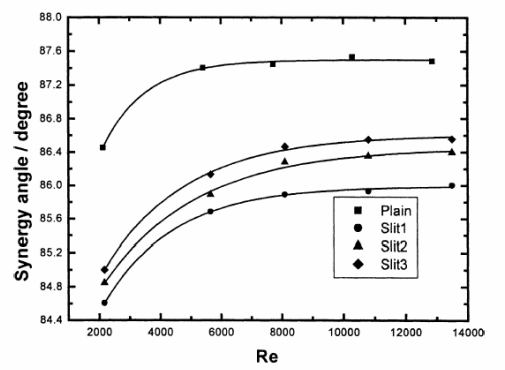

Fig. 32 Synergy angle vs Re for the four types of fins

Experiments were conducted for two heat exchangers, one with plain plate fin and the other with the slotted fin of version 1(Fig. 30(b)). The overall heat transfer coefficients and the air-side pressured data are presented in Fig. 33. Compared with the heat exchanger with plain plate fin, the increase in the overall heat transfer coefficient of the slotted fin heat exchanger is at least 26%, while the increase in air side pressure drop is at most 22%, showing very good performance of the designed fin surface.

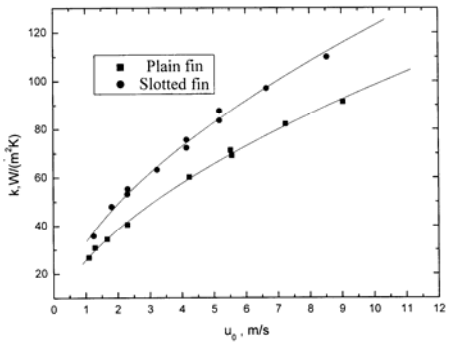

(a) Overall heat transfer coefficient

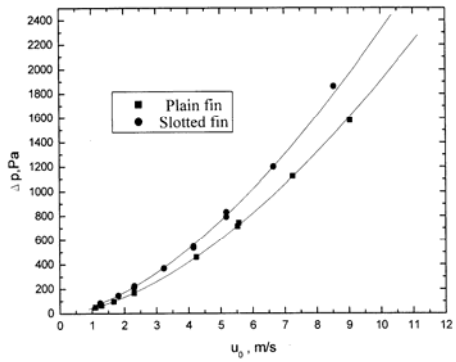

(b) Air side pressure drop

Fig. 33 Test results for the selected slotted fin surface

6.2 Centre-Blocked Longitudinal Finned Tube

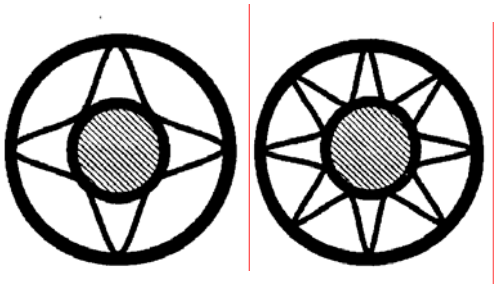

(a) Four waves (b) Eight waves

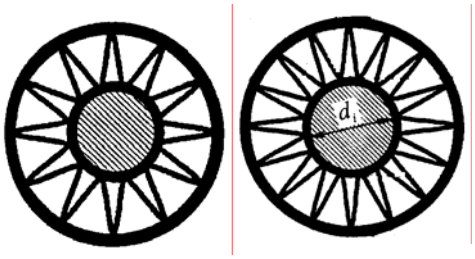

(c) Twelve waves (d) Twenty waves

As proved in section 3 the blockage of tube centre may improve the synergy of fluid temperature gradient and velocity, hence enhance the heat transfer between tube wall and fluid moving in the annular space. To further enhance the heat transfer longitudinal fins were used which sit on the outside surface of the blockage. In order to get an almost optimum configuration for enhancing heat transfer with mild pressure drop penalty, tubes with different wave numbers were manufactured (Fig. 34), and both experimental measurements and numerical simulations were conducted [34]. Numerical simulations were conducted only for the fully developed region, while measurements were for both entrance and full fully developed regions. A typical measurement result are presented in Fig.35. From the numerical simulations and test results, it is found that the tube with 20 waves has the best performance. The performance comparisons show that compared with a longitudinally finned tube without blockage, this tube can enhance heat transfer by 26% ~ 40%, while the pressure drop increase is only by 5.8% ~ 11%(Figs. 36).

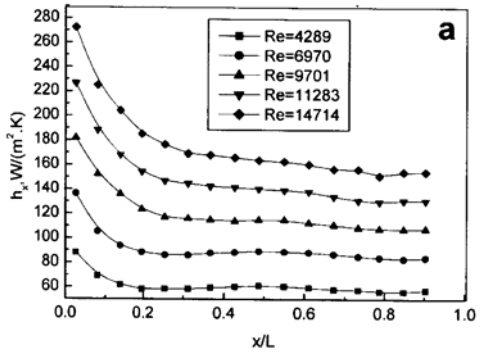

Fig. 35 Test data for tube with 20 waves

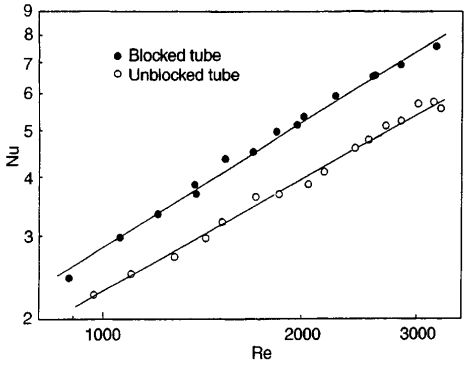

(a) Comparison of Averaged Nusselt number

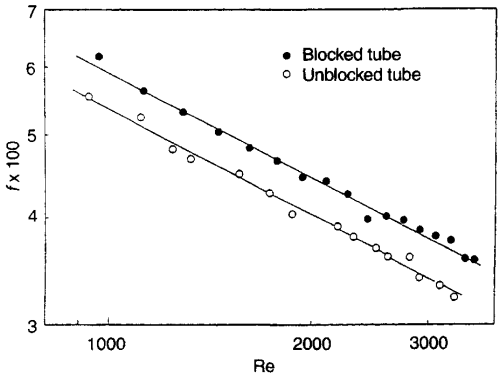

(b) Comparison of Averaged friction factor

Fig. 36 Comparisons of blocked and unblocked tubes

6.3 Alternatively Twisted Elliptic tube

For internal flow in ducts, heat transfer mainly occurs in cross sections, hence, improve the synergy between cross sectional velocity and temperature gradient is of crucial importance. The velocity field in the duct cross section can be varied by changing the duct configuration. A special tube (Fig. 37), called alternatively twisted elliptic tube (ATET), is designed for such purpose [35].

(a) Picture of ATET

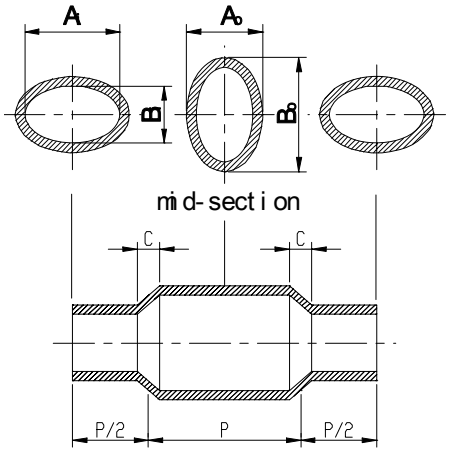

(b) Cross section views

Fig. 37 Alternating elliptical axis tubes

Both experimental measurements and numerical simulations were performed for revealing the fluid flow and heat transfer characteristics of ATET. Figure 38 gives the comparison results for the Nusselt number and friction factor between the test results for water and lubricating oil of the enhanced tube (denoted by Nue and fe) and a smooth circular tube (denoted by Nus and fs)[35]. It can be seen that a great enhancement can be made with a reasonable increase in the friction, and for the laminar flow case, the ratio of heat transfer enhancement is even much larger than that of the friction factor increase. It reveals by numerical simulation for water [35] that at each cross section there are several vortices which significantly improve the synergy between the velocity and the temperature field (Fig. 39). For a straight elliptic tube there is no such vortex formed in the cross section and the isothermals are basically elliptical. Thus the cross section synergy between velocity and temperature field is much worse, and hence the heat transfer.

In order to further confirm above discovery, numerical simulations were performed for air flow in ATET and in elliptical tube with constant wall condition [36]. The cross sectional velocity and isothermal distribution of fully developed fluid flow and heat transfer at Re = 20000 are presented in Fig. 40. Compared with the conventional elliptical tube, the synergy improvement in ATET can be clearly observed.

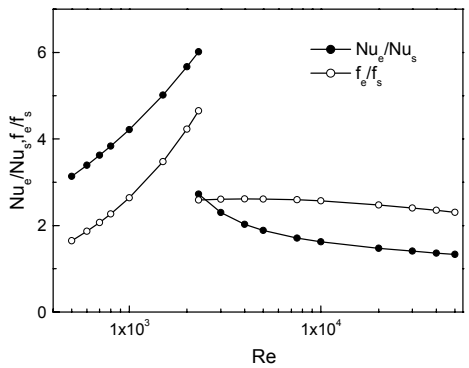

Fig. 38 Comparison of ATET and smooth circular tube

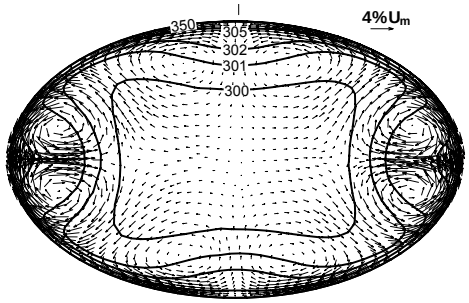

Fig. 39 Cross section water velocity and isothermal distribution of ATET

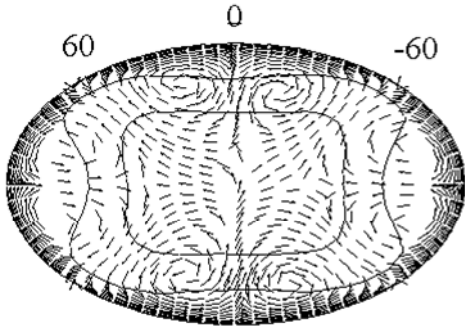

(a) ATET

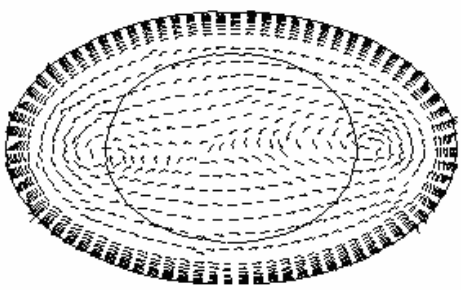

(b) Elliptical tube

Fig. 40 Air velocity and isothermal distribution for ATET and elliptical tube at a cross section

7. CONCLUSIONS

(1) The field synergy principle reveals the fundamental mechanism for enhancing single phase convective heat transfer, which can unify all existing explanations for the single phase convective heat transfer. All the existing enhancement techniques for single phase flow finally lead to the improvement of the synergy, i.e., the reduction of the intersection angle between velocity and fluid temperature gradient.

(2) The field synergy principle provides very useful rule to improve surface structure for a better heat transfer performance. The enhancement techniques should be positioned in those places where the synergy are much worse than the other place. Local synergy angle is a useful indication to reveal such places.

(3) Numerical simulation is very useful in revealing where

synergy is worse and where the enhancement techniques should be added. In conjunction with some necessary experimental measurements, numerical simulation can play an important role in the development of new types of enhanced structures with high performance.

ACKNOWLEDGMENTS

The work is supported by the following Chinese foundations: (1) National Natural Science Foundation of China (No. 50636050, 50425620, 50476046);(2) Fundamental Key Project of R & D of China (2007CB206902)

REFERENCES

[1]. A.E.Bergles. Heat transfer enhancement - the maturing of the second generation heat transfer technology. *Heat transfer Engineering*, Vol. 18, 1997, pp. 47-55.

[2]. A.E.Bergles. Heat transfer enhancement-the encouragement and accommodation of high heat fluxes. A*SME J. Heat Transfer*. Vol. 119, 1997,pp. 8-19.

[3]. A.E.Bergles. Techniques to enhance heat transfer. In:W.M.Rohsenow, J.P.Hartnett, Y.I.Chi (eds). *Handbook of Heat Transfer*,3rd ed. McGraw-Hill, New York, 1998, pp. 11.1-11.76

[4]. A.E.Bergles. Enhanced heat transfer:endless frontier, or mature and routine. *Journal of Enhanced Heat Transfer*, Vol. 6, 1999, pp. 79-88.

[5]. R.L.Webb. *Principles of Enhanced Heat Transfer,* John Wiley & Sons Inc., 1999. p.89

[6]. F.P. Incropera, D.P. DeWitt. *Fundamentals of Heat and Mass Transfer*. John Wiley & Sons, New York 2002, 356

[7]. Y.A.Cengel. Heat Transfer, *A Practical Approach*, WCB McGraw-Hill, Boston.1998,p.378

[8]. Y.N.Lee. Heat transfer and pressure drop characteristics of an array of plates aligned at angles to the flow in a rectangle duct. *Int. J. Heat Mass Transfer*. 1986, 22: 1553-1563

[9]. L.B.Wang, G.D.Jiang, W.Q.Tao, H.Ozoe. Numerical simulation on heat transfer and fluid flow characteristics of arrays with non-uniform plate length positioned obliquely to the flow direction. *ASME J. Heat Transfer*, Vol. 120, 1998, pp. 991-998.

[10]. B.Yu, J.H.Nie and W.Q.Tao. Experimental study on the pressure drop and heat transfer characteristics of tube with internal wave-like longitudinal fins. *Heat Mass Transfer,* Vol. 35, 1999, pp. 65-73.

[11]. Z.Y.Guo, D.Y.Li and B.X.Wang. A novel concept for convective heat transfer enhancement. *Int J. Heat Mass Transfer*, Vol. 41, 1998, pp. 2221-2225.

[12]. S. Wang, Z.X. Li, Guo Z.Y. Novel concept and device of heat transfer augmentation. *In proceedings of 11th IHTC*, Vol.5, 1998,pp. 405-408.

[13]. D.B.Guralinik. editor-in-chief. *Webster New World Edition,* William Collins Publishers, Inc. Cleveland.1979, p.1444.

[14]. W.Q.Tao, Z.Y.Guo and B.X.Wang. Field synergy principle for enhancing convective heat transfer - its extension and numerical verification. *Int. J. Heat Mass transfer*, Vol.45, 2002, pp.3849-3856.

[15]. Kays W M, Crawford, M E. *Convective heat and mass transfer,* New York: McGraw-Hill Company, 1980, 107,246

[16]. Z.Y.Guo, W.Q.Tao and R.K.Shah. The field synergy (coordination) principle and its applications in enhancing single phase convective heat transfer. Int J. Heat Mass Transfer, Vol. 48, 2005, pp. 1797-1807.

[17]. F.Q.Song , Z.G.Q, Y.L.He and W.Q.Tao. Numerical study of heat transfer of air across finned tube at low speed. Journal of Xi'an Jiaotong University, Vol.36, No. 9, 2002 , pp. 899-902.

[18]. M.H. Shi, H. Wang and Y.L.Hao. Study on forced convective heat transfer in centrifugal fluidized bed , *Journal of Engineering Thermophysics,* Vol. 23, No.4 2002, pp. 473-476.

[19]. M. Zeng, W.Q.Tao. Numerical verification of the field synergy principle for turbulent flow. *Journal of Enhanced Heat Transfer,* Vol. 11, No.4, 2004, pp. 451-457.

[20]. Z.Y.Li. Study on turbulent flow and heat transfer in rotating channels. PhD thesis, Xi'an Jiaotong University, Xi'an, China, 2001

[21]. G. B. Schubauuer, W. G. Spangenberg, Forced mixing in boundary layers, *J. Fluid Mech,* Vol. 8, 1960, pp. 10-31.

[22]. T. R. Johnson, P. N. Joubert, The Influence of vortex generators on drag and heat transfer from a circular cylinder normal to an airstream, *ASME J. Heat Transfer* Vol. 91, 1969, pp. 91-99.

[23]. M. Fiebig and M.A. Sanchez, Enhancement of heat transfer and pressure loss by winglet vortex generators in a fin–tube element, *HTD-Vol.*201, pp4-14, ASME, New York, 1992.

[24]. G. Biswas, N.K. Mitra, M. Fiebig, Heat transfer enhancement in fin-tube heat exchangers by winglet type vortex generators, *Int. J. of Heat Mass Transfer,* Vol. 37, 1994, pp. 283-291.

[25]. Y. Chen, M. Fiebig, N.Y. Mitra, Heat transfer enhancement of a finned oval tube with punched longitudinal vortex generators in-line, *Int. J. of Heat Mass Transfer,* Vol. 41 , 1998, pp. 4151-4166.

[26]. Y. Chen, M. Fiebig, N.Y. Mitra, Heat transfer enhancement of a finned oval tubes with staggered punched longitudinal vortex generators, *Int. J. of Heat Mass Transfer*, Vol.43, 2000, pp. 417-435.

[27]. J.S. Leu, Y.H. Wu, J.Y. Jang, Heat transfer and fluid flow analysis in plate-fin and tube heat exchanger with a pair of block shape vortex generator, *Int. J. of Heat Mass Transfer*, Vol. 47, 2004, pp. 4327-4338.

[28]. J. M. Wu, W. Q. Tao. Investigation on laminar convection heat transfer in fin-and-tube heat exchanger in aligned arrangement with longitudinal vortex

generator from the viewpoint of field synergy principle. *Applied Thermal Engineering*, in press

[29]. J. M. Wu, W. Q. Tao. Numerical study on laminar convection heat transfer in a rectangular channel with longitudinal vortex generator Part A: Verification of field synergy principle. *International Journal Heat Mass Transfer*, in press.

[30]. Y.L.He, Z.G.Qu and W.Q.Tao. New Understanding of Convective Heat Transfer Enhancement and Its Engineering Applications. Heat Transfer Engineering, Accepted

[31]. L.D.Ma, W.Q.Tao and Y.L.He. Heat transfer in ducts with velocity normal to temperature gradient-experimental validation of field synergy principle. *International Communications in Heat Mass Transfer*, in press.

[32]. Tao WQ, He YL, Wang QW, Qu ZG, Song FQ. A unified analysis on enhancing single phase convective heat transfer with field synergy principle. *Int J Heat Mass Transfer*, 45 (24): 4871-4879 2002,

[33]. Y.P. Cheng, Z.G. Qu, W.Q. Tao, and Y.L. He. Numerical design of efficient slotted fin surface based on the field synergy principle. *Numerical Heat Transfer,* Part A, Vol. 45, 2004, pp. 1-22.

[34]. B. Yu, W. Q. Tao. Pressure drop and heat transfer characteristics of turbulent flow in annular tubes with internal wave-like longitudinal fins. *Heat Mass Transfer*, Vol. 40, No. 8, 2004, pp. 643-651.

[35]. J.A. Meng. Enhanced heat transfer technology of longitudinal vortices based on field-coordination principle and its application. *Ph D. Thesis*, Tsinghua University, Beijing, China, 2003.

[36]. B. Li , B. Feng, Y. L. He and W. Q. Tao. Experimental study on friction factor and numerical simulation on Flow and heat transfer in an alternating elliptical axis tube. *Applied Thermal Engineering,* Vol. 27, 2006, pp. 365-372.